

Adsorption of metal adatoms on FeO(111) and MgO(111) monolayers: Effects of charge state of adsorbate on rumpling of supported oxide film

Jacek Goniakowski,^{1,*} Claudine Noguera,¹ Livia Giordano,² and Gianfranco Pacchioni²

¹CNRS, INSP, UMR 7588, and Université Pierre et Marie Curie, Campus de Boucicaut, 140 Rue de Lourmel, 75015 Paris, France

²Dipartimento di Scienza dei Materiali, Università di Milano-Bicocca, via Cozzi, 53-20125 Milano, Italy

(Received 24 April 2009; revised manuscript received 30 July 2009; published 4 September 2009)

We present a theoretical density-functional theory study on the deposition of metal atoms (Ir, Pd, Pt, Ag, and Au) on FeO(111) and MgO(111) monolayers supported on Pt(111). We show the existence of a strong coupling between the charge state of the adsorbed adatom and the local polaroniclike distortion of the oxide film, and we identify two qualitatively different adsorption modes in which the distortion either reinforces the rumpling of the supported oxide film (positively charged adsorbates) or reduces or even reverses the cation-anion stacking (negatively charged adsorbates). Thus, the adsorption mode is a response to the charge state of the adsorbate and is driven mainly by the capacity of adatoms to exchange electrons with the support.

DOI: [10.1103/PhysRevB.80.125403](https://doi.org/10.1103/PhysRevB.80.125403)

PACS number(s): 68.43.Fg, 64.70.Nd, 68.55.aj, 73.61.Ng

I. INTRODUCTION

Metallic particles grown on oxide supports are relevant in heterogeneous and environmental catalysis^{1–4} and factors determining their reactivity have been under investigation from both fundamental and applicative points of view. The basic research in model catalysis has adopted thin oxide films as supports,⁵ which, beyond a critical thickness, behave like bulk oxide surfaces but at the same time offer the advantage to avoid charging phenomena connected to the use of photoelectron spectroscopies. However, it has become clear in recent years that supported ultrathin oxide films may exhibit unique properties, different from their bulk counterparts, in particular, concerning the charge state of adsorbed species: a property of crucial importance for the growth, chemical, optical, and magnetic properties of the metal particles.^{5,6}

The ability to promote spontaneous electron flow through an ultrathin oxide film has been first proposed theoretically,^{7–11} and later confirmed experimentally.^{12,13} For Au atoms^{7,8,10} deposited on ultrathin MgO films supported on Mo(100) or Ag(100) substrates, electrons flow from the metal substrate to the deposited gold by direct tunneling through the oxide thin film. A similar effect has been found on alumina films on NiAl(110), where deposited gold forms negatively charged chains due to the formation of direct Au-Al bonds.^{14,15} So far, mostly negative Au atoms and particles have been observed on metal-supported oxide films. Only recently it has been shown that on the well-characterized FeO/Pt(111) support,^{16–21} self-organization of Au adatoms is observed²² and electron transfer results in a positive charge of Au adatoms.²³ The occurrence of positive charging has also been predicted for alkali metals on oxide thin films.^{8,24,25}

While the metal/oxide interface determines the electronic characteristics (e.g., the work function) of the support and, thus, its capacity to exchange electrons with the adsorbates, atomic relaxation of the oxide film may significantly contribute to stabilize charged adsorbates (polaroniclike effect). Due to their structural flexibility, this effect becomes particularly important on ultrathin films of insulating materials. It has been shown that charged species can be stabilized on NaCl

and MgO ultrathin films, due to strong local structural rearrangements.^{7,8,26,27} Other examples have been reported for Au atoms and clusters deposited on alumina and titania thin films.^{14,15,28,29} In this latter case, the particular adsorption characteristics were tentatively assigned to the polar orientation of the supported film.

Structural relaxation in supported oxide films becomes of crucial importance in the limit of a monolayer. Some of us have recently shown³⁰ that the rumpling of supported oxide monolayers is electrostatically coupled to the electronic characteristics of the metal substrate. The rumpling is defined as the separation between the atomic planes of cations and anions of the monolayer. In general, while no rumpling is found for the unsupported monolayer films,³¹ a substantial rumpling is observed when films are supported on metal substrates. We have argued that while the substrate electronegativity determines the sign and extent of the charge transfer (CT) at the metal/oxide interface, this latter induces an electric field which drives the rumpling of the oxide film. When oxide films are deposited on substrates of high electronegativity, oxide films donate electrons to the metal substrate and the anions are repelled outward [Fig. 1(a)]. Conversely, on substrates with low electronegativity, electrons flow from the metal to the oxide and the cations are repelled outward [Fig. 1(b)]. In this respect, the rumpling in the supported film can be seen as a structural response to the occurrence of a charge transfer between the oxide and the metal substrate. Dipole moment associated to the rumpling in the oxide film (D_R) opposes and partially compensates that due to charge transfer at the interface (D_{CT}).

For similar reasons, upon deposition of metal atoms on supported oxide films, the electron flow between the adatom and the metal/oxide support is expected to produce local distortions in the oxide monolayer. The goal of the paper is to extend the scenario described above to adatom adsorption on metal/oxide supports and to rationalize the computed trends in terms of basic properties of the system. In this way, we provide guidelines for the experimental fabrication and tuning of these systems. We will highlight the relationship between the charge state of the adsorbate Q_{ads} and the adsorption-induced local structural modification of the oxide

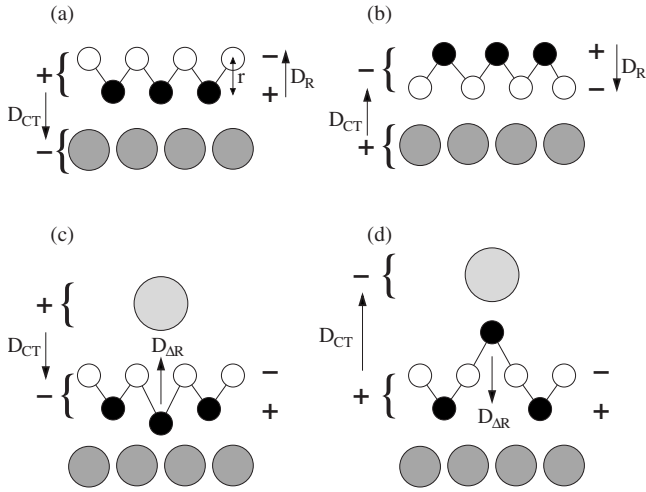


FIG. 1. (a) and (b) Schematic representation of the interface charge transfer (D_{CT}) and oxide film rumpling (D_R) dipole moments in bare oxide monolayer films (black circles cations, white circles anions) with positive (a) and negative (b) rumpling r deposited on a metal substrate (large gray circles). (c) and (d) Schematic representation of “direct” (c) and “flipped” (d) adsorption modes of an adatom (large circle) on a supported oxide film. In direct adsorption, the polaroniclike distortion induced by the adatom increases locally the rumpling (distance between planes of anions and cations); in flipped adsorption mode, the distortion locally reduces or inverts the rumpling. Dipole moments due to charging of the adatom (D_{CT}) and to the adsorption-induced structural distortion (D_{AR}) are plotted schematically with arrows in the two cases.

support. We will identify two qualitatively different adsorption modes, in which the adsorption-induced local distortion either reinforces the rumpling of the supported oxide film [Fig. 1(c)] or reduces or even inverts it [Fig. 1(d)]. The adsorption mode will be described as a structural response of the oxide film to the charge state of the adsorbate, mainly driven by the ability of the adatoms to exchange electrons with the support. Similarly to the case of the supported bare oxide film, dipole moment associated to the local modification of rumpling in the oxide film (D_{AR}) opposes and partially compensates that due to charge transfer between the substrate and the adsorbate (D_{CT}).

For the sake of generality, we will focus on trends obtained for a series of isolated adatoms of different electronic properties (Ir, Pd, Pt, Ag, and Au) adsorbed on Pt(111)-supported MgO(111) and FeO(111) monolayers. We will show that our proposed scenario holds equally well for strongly ionic MgO and more covalent reducible FeO, where also the transition-metal cations are involved in the adsorption process. The high work function of Pt(111) offers the opportunity to stabilize both negative and positive adsorbates even of highly electronegative elements such as late transition and noble metals used in experiments.

II. COMPUTATIONAL METHOD

For the calculations, we use the density-functional theory (DFT) approach (MgO case) and the DFT+ U approach (FeO case) ($U_{Fe} - J_{Fe} = 3$ eV), as formulated by Dudarev *et al.*³²

and implemented in the VASP code,^{33,34} with the generalized gradient approximation and the Perdew-Wang 91 functional³⁵ [plane-wave basis set with kinetic-energy cutoff of 400 eV, with ultrasoft pseudopotentials (MgO case) and projector augmented wave method^{36,37} (FeO case)]. All oxide/metal systems are represented by Pt(111) slabs composed of five atomic layers with one bare metal surface and one covered with oxide separated by a vacuum layer of about 11 Å. The oxide/Pt(111) interface is modeled with a non-pseudomorphic periodic unit cell obtained by a superposition of $(\sqrt{3} \times \sqrt{3})R30^\circ$ -oxide(111) and (2×2) -Pt(111) structures. This interface model [at FeO(111) experimental lateral lattice parameter of 3.1 Å] includes the three characteristic sites of the experimental Moiré unit cell (Fe-top, Fe-hcp, and Fe-fcc)¹⁹ and reproduces satisfactorily the main features reported in the recent study of adatom adsorption on the FeO/Pt(111) support.²³ For comparative purposes, the same interface model has been used for MgO/Pt(111); as lateral lattice parameter we used the equilibrium lattice parameter of Pt-supported MgO monolayer 3.3 Å, determined as the minimum of the total-energy difference between MgO/Pt(111) and Pt(111) subsystems computed as a function of lateral lattice parameter.³⁰ Such a procedure eliminates the first-order contribution due to the metal distortion and minimizes essentially the energy of the oxide film augmented by the interaction energy at the metal/oxide interface. In practice, for each fixed value of the lateral lattice parameter, all inter-layer distances were allowed to relax (residual forces smaller than 0.01 eV/Å), so that the residual stress due to the lattice mismatch is accommodated by a full relaxation of the inter-layer spacing in the Pt(111) slab.

Two adsorption geometries for an isolated metal adatom (a single adatom per unit cell) have been considered: on top of oxygen anions [anions of the oxide film are in hcp sites with respect to the Pt(111) surface] and on top of metal cations (cations of the oxide film are on top of the Pt atoms of the substrate). We did not consider other less symmetric adsorption geometries [e.g., bridge and hollow adsorption sites in the case of Pd/FeO/Pt(111) (Ref. 23)], but for the systems considered the corresponding energy differences are small and do not alter the discussed trends. We report Bader charges of atoms and ions,^{38,39} but we remind that the corresponding absolute values may suffer from the arbitrariness typical of every charge decomposition scheme. This may apply also to the comparisons of charge values for systems with a significantly different bonding nature. We will also discuss results obtained for a fixed value of the distortion. In these cases, the vertical distance between anionic and cationic atomic layers has been constrained globally (bare oxide monolayer) or locally at the adsorption site (adatom adsorption).

The electronic characteristics of free metal atoms considered in the present study are quantified by the mean values $(IP+EA)/2$ of their calculated ionization potentials (IP) and electronic affinities (EA). IP and EA are estimated as total-energy differences of neutral and charged isolated atoms obtained in calculations performed in a cubic 15 Å large supercell. Dipole corrections are systematically applied and a neutralizing homogenous background is added in calculations of charged species.

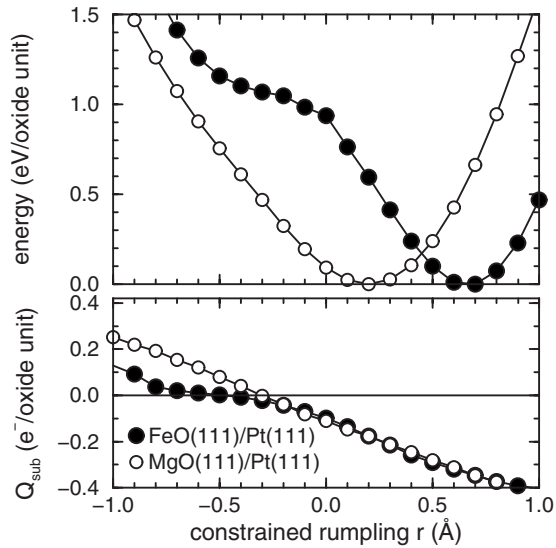


FIG. 2. Total energy (eV/oxide unit) and charge transfer at the metal/oxide interface Q_{sub} (electron/oxide unit) for bare FeO(111) and MgO(111) films supported on the Pt(111) surface, as a function of the constrained rumpling r of the oxide film. Positive rumpling corresponds to oxygen relaxing outward. Positive Q_{sub} represents an electron flow from the metal substrate to the oxide film.

III. RESULTS

Rumpling of bare oxide layers. We first consider the properties of bare Pt(111)-supported oxide monolayers (Fig. 2): the total energy per oxide formula unit and the interfacial charge transfer Q_{sub} [charge at the Pt(111) substrate per oxide formula unit] are reported as a function of the rumpling in the oxide film. A positive rumpling (as measured by the average distance $\langle r_0 \rangle$ between the cation and anion planes) corresponds to the oxide anion moving outward; a negative rumpling to a cation displacement outward. The charge Q_{sub} is defined positive when electrons flow from the metal support to the oxide.

While perfectly flat when self-standing^{20,31} (no rumpling), both MgO(111) and FeO(111) monolayers undergo a positive rumpling when supported on the Pt(111) substrate, with average $\langle r_0 \rangle = 0.66$ Å for FeO(111) and 0.14 Å for MgO(111). We note that the above average value $\langle r_0 \rangle$ for MgO is somewhat smaller than the estimation obtained in calculations with a constrained uniform rumpling in the oxide film [(Fig. 2) the same rumpling was imposed throughout the whole oxide film, independently of the local register with the substrate]. As it has been shown in Ref. 30, the rumpling in the oxide film is not due to the lateral strain in the oxide film but originates from electronic effects due to charge transfers at the interface. Indeed, the high electronegativity of the Pt substrate favors an electron flow from the oxide film toward the metal for both unrelaxed and relaxed films [$Q_{\text{sub}}(r=0) < 0$ and $Q_{\text{sub}}(\langle r_0 \rangle) < 0$ (Fig. 2)]. The electric field generated by Q_{sub} repels the oxygen atoms and induces a positive rumpling $r > 0$ with an associated dipole moment, which opposes and partially cancels that due to the charge transfer [Fig. 1(a)]. The negative rumpling with cations relaxed outward [Fig. 1(b)] is not expected for oxides on Pt but could occur in systems which favor charge flow toward the oxide layer,

hence, a positive charging of the metal substrate, such as, for instance, for metals with low electronegativity. In the case of reducible FeO(111), one can indeed identify a hint of this second solution at $r \sim -0.25$ Å, where the curve seems to indicate the occurrence of a crossing between two different states. This solution however remains much less stable energetically.

Due to the prevalence of the electronic compression contribution (Pauli repulsion), the computed total dipole moment corresponds to a reduction in the metal work function.^{30,20,40} It amounts to -0.6 eV and -0.9 eV for FeO and MgO films, respectively, resulting in a somewhat lower work function for the MgO/Pt(111) support.⁴¹

Adsorption of isolated adatoms. Previous studies on Au adatoms on FeO/Pt(111) have shown the occurrence of a significant local distortion of the oxide film.²³ When Au is bound on top of O anions of the FeO monolayer, the rumpling of the oxide film increases locally by about 20%. When Au is adsorbed on top of Fe cations, the effect is opposite, as the Fe ion directly below the Au atom moves from the interface outward and stands above the oxygen plane in the final “flipped” configuration [Fig. 1(d)]. These two different adsorption modes are associated to an opposite charge of the gold adatom, positive on top of O anions and negative on top of Fe cations. On the contrary, for Pd on the same support only the “direct” configuration is stable and the adsorption results in a small increase in rumpling of the FeO film [Fig. 1(c)].²³ In the following, we will try to rationalize this behavior in a more general context by comparing various adsorbed metal atoms, two oxide films FeO/Pt(111) and MgO/Pt(111), and by analyzing the relationship between the local distortion and the charge of the adsorbed atoms.

Figure 3 displays the adsorption properties of isolated adatoms on FeO/Pt(111) and MgO/Pt(111) supports. In particular, we focus on the charge of the adsorbate Q_{ads} (a negative Q_{ads} corresponds to electron transfer from the support to the adatom) and on the local change in the equilibrium rumpling of the oxide film induced by the adatom $\Delta \langle r_{\text{eq}} \rangle = \langle r_{\text{eq}} \rangle - \langle r_0 \rangle$ ($\langle r_0 \rangle$ and $\langle r_{\text{eq}} \rangle$ represent the average equilibrium rumpling of the fully optimized supported oxide film, bare, and in the presence of an adsorbate, respectively). Due to averaging over the entire surface unit cell, $\Delta \langle r_{\text{eq}} \rangle$ enables a simple quantification of the otherwise complex local distortion induced by the adatom. Indeed, while in most of the considered cases this distortion is mainly limited to the adsorption site only, we find that, in some cases, it may also affect first and more distant neighbors. For example, it extends to first neighbors in the case of Ir and Pt adsorption on MgO(111) and involves all ions in the surface unit cell in the case of Au/MgO(111). Finally, we note that with this definition $\Delta \langle r_{\text{eq}} \rangle$ is not biased to a particular type of adsorption site only and can be systematically used for all adatom configurations.

The two quantities Q_{ads} and $\Delta \langle r_{\text{eq}} \rangle$ are plotted as a function of the mean value $(\text{IP} + \text{EA})/2$ of the calculated IP and EA of the free atoms, which increases along the series $\text{Ag} < \text{Pd} < \text{Ir} < \text{Pt} < \text{Au}$. This scale is qualitatively similar to the Pauling electronegativity scale.⁴² The different nature of the two oxides, the different degree of covalence of the adsorbate-oxygen bond, and the different character of

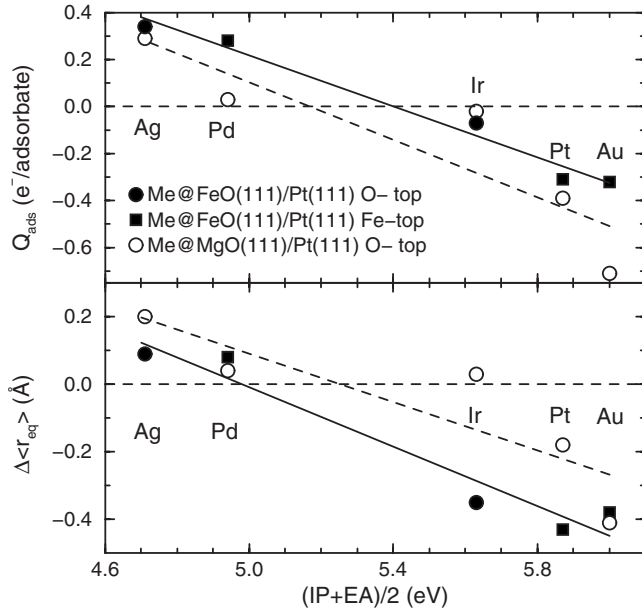


FIG. 3. Charge of metal adatom Q_{ads} (electron/adsorbate) and adsorbate-induced distortion of the oxide film $\Delta\langle r_{\text{eq}} \rangle$ (Å), as a function of calculated atomic properties of the adsorbate (average of the ionization potential and the electronic affinity). Lines are drawn to guide the eyes.

adsorbate-cation interaction result in different preferential adsorption sites. While adsorption on top of oxygen is systematically favored on MgO/Pt(111), in the case of FeO/Pt(111) support, we find a preference for the on-top Fe site for Pd, Pt, and Au, while Ir and Ag adsorb on top of oxygen. Results reported in Fig. 3 refer to these preferential adsorption sites.

Figure 3 evidences the existence of a direct correlation between the electronic (Q_{ads}) and structural ($\Delta\langle r_{\text{eq}} \rangle$) properties of the systems and the adatom electronegativity. The adatoms under consideration can be grouped into two families characterized by a qualitatively different adsorption mode. While adsorbates with a low electronegativity, such as Ag and Pd [small $(IP+EA)/2$ values] become positively charged ($Q_{\text{ads}} \geq 0$) and moderately alter the oxide structure (direct adsorption mode shown in Fig. 1(c): $\Delta\langle r_{\text{eq}} \rangle$ positive but small), adatoms that accept electrons more easily, such as Au and Pt [large $(IP+EA)/2$ values] become negatively charged ($Q_{\text{ads}} \leq 0$) and induce a more pronounced effect on the local rumpling by reducing or even reversing it ($\Delta\langle r_{\text{eq}} \rangle < 0$). This latter configuration corresponds to the flipped adsorption mode described above and shown in Fig. 1(d). Iridium adsorption constitutes an intermediate case, with a particular small charge transfer at both substrates. Ir deposition on FeO/Pt(111) follows the trend described above (same signs of $\Delta\langle r_{\text{eq}} \rangle$ and Q_{ads}) but deviates from it on MgO/Pt(111). We note however that in this latter case, both $\Delta\langle r_{\text{eq}} \rangle$ and Q_{ads} are particularly small and, thus, both their signs and precise values may be particularly sensitive to the constraints of the calculations. Finally, we note that the above relation between electronic and structural properties of the systems and the adatom electronegativity is only little sensitive to the precise nature of adatom bonding. Indeed, in the case of the

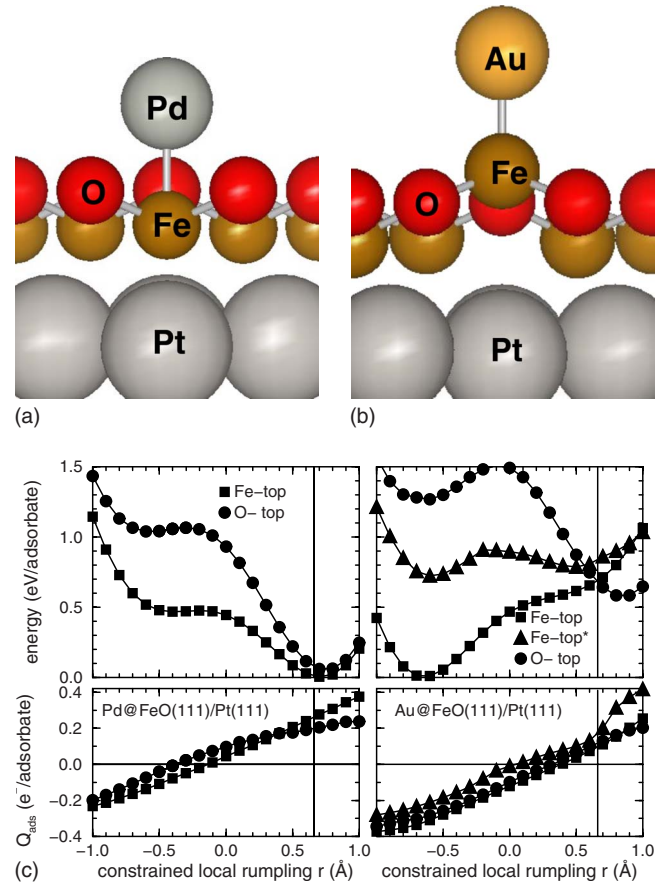


FIG. 4. (Color online) Relative energy (eV/adsorbate) and net charge Q_{ads} (electron/adsorbate) of adsorbed Pd and Au adatoms as a function of the constrained local rumpling r of the FeO(111) film. Positive values of r correspond to oxygen relaxing outward. Vertical line indicates average equilibrium rumpling in a bare supported oxide film $\langle r_0 \rangle$. Both Fe-top and O-top adsorption geometries are considered. Fe-top* data refer to results obtained with an artificial modification of the Au properties, in particular, to a lower value of $(IP+EA)/2$ (see text for details).

FeO/Pt support [Fig. 3], the same trend is followed by both Fe-top and O-top configurations.

IV. DISCUSSION

To better understand this relationship, in Figs. 4 and 5 we report the relative energy and adsorbate charge Q_{ads} as a function of the local distortion r of the film for two adatoms representative for the two adsorption modes: Pd, with a smaller calculated $(IP+EA)/2$ value of 4.9 eV (direct adsorption mode) and Au with $(IP+EA)/2$ of 6.0 eV (flipped adsorption mode). We consider a constrained local distortion, where only the rumpling at the adsorption site is fixed to a given value r and the rest of the oxide film, the adatom, and the Pt substrate are free to relax (as opposed to the averaged “equilibrium” rumplings $\langle r_{\text{eq}} \rangle$ and $\langle r_0 \rangle$ issued from unconstrained optimization of all structural degrees of freedom). Positive values of r correspond to an outward oxygen relaxation. The values of rumpling in the corresponding bare supported oxide films $\langle r_0 \rangle$ are indicated by vertical lines, allow-

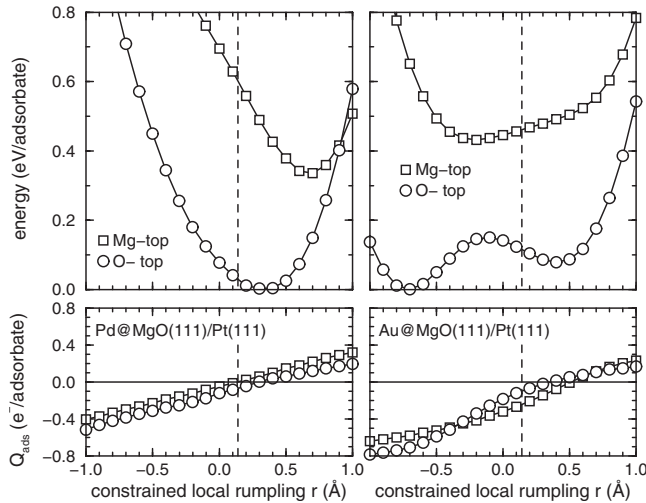


FIG. 5. Same as Fig. 4 for Pd and Au adatoms adsorbed on the MgO(111)/Pt(111) support.

ing the estimation of $\Delta r = r - \langle r_0 \rangle$. Adsorption on top of O and on top of the metal cation (Mg or Fe) has been considered.

The global minima reproduce well the results presented already in Fig. 3: on both substrates Au charges negatively and adsorbs preferentially in the flipped mode ($\Delta r_{\text{eq}} < 0$), while Pd charges positively and adsorbs in the direct mode ($\Delta r_{\text{eq}} > 0$). Figures 4 and 5 display also local minima on the potential-energy curves. For instance, Au adsorbed on top of O on FeO/Pt(111) is positively charged (see Ref. 23); the total energy of this minimum is about 0.6 eV higher than on top of Fe (Fig. 4). On-top oxygen adsorption of Au on MgO/Pt(111) produces a local minimum only 0.1 eV above the global one; in this metastable state Au is slightly positively charged and the rumpling is enhanced (Fig. 5). Finally, in most cases, global and local minima are separated by energy barriers. While they are partly due to the constraints imposed to fix the local rumpling, more generally finite barriers may indeed be expected especially in cases of a strong rumpling of the bare supported oxide film, such as, e.g., FeO(111)/Pt(111).

In summary, regardless of the oxide, the adatom, and the adsorption site, Q_{ads} varies in a quasilinear way with the local distortion r . Moreover, independently of the overall stability of a configuration (global or local minimum), a positively charged adsorbate is always associated to the direct adsorption mode and a negatively charged adsorbate to the flipped mode, so that Δr and Q_{ads} have the same sign.

These results can be accounted for by extending the arguments used for the analysis of rumpling in bare metal-supported oxide films (Ref. 30). Here, the support-adsorbate charge transfer Q_{ads} may be viewed as an electronic response of the system to the energy separation (δE) between the Fermi level of the oxide/metal support (E_F) and the donor or acceptor level of the adsorbate (ε_{ads}): $\delta E = E_F - \varepsilon_{\text{ads}}$ modified by the dipole moment induced by adatom adsorption (D_{ads}),^{30,42}

$$Q_{\text{ads}} = -\chi(\delta E - D_{\text{ads}}), \quad (1)$$

where χ is the electronic susceptibility of the interface and is related to the optical dielectric function. D_{ads} includes a CT

contribution ($D_{\text{CT}} \sim -Q_{\text{ads}} \cdot R_{\text{ads}}$, where R_{ads} is the distance between the adsorbate and the oxide film) and a contribution due to the modification of film rumpling ($D_{\Delta R} \sim Q \cdot \Delta r$, where $Q > 0$ is the absolute value of the charges of the ions in the oxide layer). Thus, the solution of the implicit Eq. (1) for a fixed Δr is

$$Q_{\text{ads}}(\Delta r) = -\kappa(\delta E - Q \cdot \Delta r), \quad (2)$$

with $\kappa = \chi / (1 + \chi R_{\text{ads}})$. Equation (2) gives grounds to the linear behavior of Q_{ads} as a function of Δr found numerically (Figs. 4 and 5).

The adsorption-induced distortion Δr_{eq} of the oxide film, corresponding to the equilibrium adsorption configuration, may be seen as due to the electric field of the charged adsorbate, which acts differently on oxide anions and cations. This electrostatic force is counterbalanced by an elastic term, which tends to restore the equilibrium rumpling $\langle r_0 \rangle$ of the bare support. To the lowest order, Δr_{eq} reads as

$$\Delta r_{\text{eq}} \propto Q Q_{\text{ads}}(\Delta r_{\text{eq}}) \propto -\delta E \quad (3)$$

and the local distortion Δr_{eq} can thus be viewed as a structural response of the oxide film to the charge transfer induced by adsorption Q_{ads} (Δr_{eq}). The related dipole moment $D_{\Delta R} \sim Q \Delta r_{\text{eq}} \sim Q_{\text{ads}}(\Delta r_{\text{eq}}) Q^2$ opposes and partially compensates that due to the charge transfer $D_{\text{CT}} \sim -Q_{\text{ads}}(\Delta r_{\text{eq}}) R_{\text{ads}}$, as schematized in Fig. 1.

Equation (3) gives grounds for understanding the direct relationship between the distortion at equilibrium $\Delta \langle r_{\text{eq}} \rangle$ and the adsorbate charge Q_{ads} found numerically (Fig. 3). Moreover, Eqs. (2) and (3) account for a more positive/less negative charging of atoms deposited on supports with a larger work function [(Me/FeO/Pt(111) versus Me/MgO/Pt(111) series in Fig. 3]. For a given support, they explain a negative charging and a flipped adsorption mode of adsorbates with high $(\text{IP} + \text{EA})/2$ values [positive δE , such as Pt or Au on both FeO/Pt(111) and MgO/Pt(111) in Fig. 3].

The influence of the atomic characteristics of adatom on the preferential adsorbed state can be further demonstrated by the results obtained for a modified Au adatom on FeO/Pt(111) (Fe top* in Fig. 4). Here we have artificially reduced the IP of the gold atom by about 0.7 eV by arbitrarily imposing $U_{\text{Au}} - J_{\text{Au}} = 8$ eV in the DFT+ U approach. In this case, we observe that the strong preference for the flipped adsorption mode is largely suppressed.

At this point, it is worth stressing that while the above model accounts for the main features of the charge transfer and film structural distortions upon adsorption, the computational results suggest that such systems may display a more complex behavior. For example, this concerns the possible multiplicity of adsorption configurations and energy barriers between them. Whether this could lead to an actual bistability, with external control by, e.g., a scanning tunneling microscope, remains to be proved and is currently under study.

While flipped adsorption configuration associated to a negative charging of Au adatoms has recently been reported on the alumina/NiAl(110) substrate,¹⁵ it is important to mention that the experimental evidence for Au atom adsorption at Pt-supported FeO(111) films²³ is consistent with positively charged adatoms and the direct adsorption mode. While a

full discussion of possible experimental and theoretical reasons of such a discrepancy goes beyond the scope of the present study, let us point out a potential source of error in computational predictions on reactivity of composite oxide/metal supports. In the present study, we have shown that the sign of adsorbate charge and the adsorption mode are directly driven by the sign of the difference δE between the Fermi level of the support and the acceptor or donor levels of the adsorbate. The precise values of these quantities are not easily obtained in the DFT approach; furthermore, the position of the Fermi level of the support may also vary as a function of the computational model of the interface.^{20,21}

Also the electrostatic interactions due to the atomic structure of the surface region (distances at the metal/oxide interface, rumpling of the oxide film) strongly affect the properties of metal/oxide supports. This may become particularly critical when the difference between the position of the Fermi level and that of the atomic states of the adsorbate δE is very small. In this case, constraints related to the size of the periodic supercell and the oxide-metal register at the interface may easily result in an opposite sign of δE compared to the real system. Finally, it should be mentioned that the strain in the metal/oxide interface may be released in different ways in experiment (e.g., formation of domain boundaries or forming incommensurate interface structures) than in calculations (expansion/contraction of the metal or oxide lattice constants).

There are two more general remarks to complete the discussion. First, in the present study we have considered a particular (polar) orientation of the oxide films. However, the simple electrostatics, which underlies the coupling between polaroniclike distortion of the support and the charge state of the adsorbate, is valid regardless of support orientation. Indeed, while a bare MgO(100) monolayer on Mo(100) presents a small electron transfer toward the metal substrate and a positive rumpling of 0.2 Å, consistent with the conclusions of Ref. 30, the deposition of Au in both the Mg-top and O-top configurations leads to a negative charging of the adatom and to a considerable (0.4 Å) local rumpling inversion, characteristic to the flipped adsorption mode.⁷ Furthermore, in a bare MgO(100) bilayer supported on Ag(100), the interfacial MgO layer is practically flat (rumpling smaller than 0.01 Å), and the surface layer shows a positive rumpling of 0.04 Å, similar to that of the bulk MgO(100) surface (0.05 Å). Upon Au adsorption on cations, the Mg atom underneath relaxes outward by 0.4 Å and the O atom of the interface layer moves downward by 0.2 Å, producing a modification of film dipole moment, which opposes the dipole moment due to the negative charging of the adatom, in agreement with the present model. Also in agreement with it is the relaxation of the opposite sign, which is observed for cationic K adsorbed on the MgO bilayer: the O atom underneath K relaxes outward by 0.4 Å, while the Mg atom of the

interface layer moves downward by 0.3 Å.⁸ As a consequence, the partial compensation of electrostatic dipoles, which takes place upon adsorption, is not a specific signature distinguishing polar and nonpolar support orientations.

Second, in the present study we have considered a highly electronegative metal substrate ($Q_{\text{sub}} < 0$), which induces a positive rumpling ($r_0 > 0$) in the two oxide films considered. The typical properties of flipped ($Q_{\text{ads}} < 0$) and direct ($Q_{\text{ads}} > 0$) adsorption modes apply to this case. However, relying on the analytical argument given above, it is easy to generalize these findings and conclude that the flipped mode occurs when the substrate and the adsorbate have charges of the same sign ($Q_{\text{sub}}Q_{\text{ads}} > 0$).

V. CONCLUSION

By studying the deposition of isolated metal adatoms (Ir, Pd, Pt, Ag, and Au) on Pt(111)-supported FeO(111) and MgO(111) monolayers, we have revealed the existence of a strong coupling between the charge state of the adsorbate and the local polaroniclike distortion of the oxide film, which results in two qualitatively different adsorption modes. The first case (direct adsorption mode) corresponds to a positive charging of the adsorbate and the rumpling of the bare oxide film is locally reinforced; the second case (flipped adsorption mode) corresponds to a negative charging of the adsorbate, and the distortion is such as to reduce or even invert the rumpling of the bare oxide film. These two adsorption modes correspond to the two ways, in which the electrostatic dipole due to the modification of the oxide structure partly compensates the dipole due to adsorbate charging. We stress that the simple electrostatics, which underlies the coupling between adsorption mode and the charge state of the adsorbate, is not specific of the polar orientation considered in the present study but holds for any kind of dielectric film. The relative stability of the two adsorption modes is driven mainly by the preferential direction of electron flow and, for a given support, it depends on the atomic properties (ionization potential, electron affinity) of the adsorbate. Since the local structural distortion of the oxide film is a response to the charging of the adsorbed atom, the present results suggest a possibility of switching between direct and flipped configurations by modifying the charge state of the adsorbate, with interesting consequences on surface properties.

ACKNOWLEDGMENTS

We thank N. Nilius for stimulating discussions and constructive comments on the present paper. We acknowledge support from the COST Action D41 *Inorganic oxides: Surfaces and interfaces*. J.G. and C.N. acknowledge support from the French ANR project *SIMINOX* Grant No. ANR-06-NANO-009-01.

*Corresponding author; jacek.goniakowski@insp.jussieu.fr

- ¹C. R. Henry, Surf. Sci. Rep. **31**, 231 (1998).
- ²C. T. Campbell, Surf. Sci. Rep. **27**, 1 (1997).
- ³H.-J. Freund, Angew. Chem., Int. Ed. Engl. **36**, 452 (1997).
- ⁴D. W. Goodman, J. Catal. **216**, 213 (2003).
- ⁵H. J. Freund, Surf. Sci. **601**, 1438 (2007).
- ⁶H. J. Freund and G. Pacchioni, Chem. Soc. Rev. **37**, 2224 (2008).
- ⁷G. Pacchioni, L. Giordano, and M. Baistrocchi, Phys. Rev. Lett. **94**, 226104 (2005).
- ⁸L. Giordano and G. Pacchioni, Phys. Chem. Chem. Phys. **8**, 3335 (2006).
- ⁹D. Ricci, A. Bongiorno, G. Pacchioni, and U. Landman, Phys. Rev. Lett. **97**, 036106 (2006).
- ¹⁰K. Honkala and H. Häkkinen, J. Phys. Chem. C **111**, 4319 (2007).
- ¹¹P. Frondelius, A. Hellman, K. Honkala, H. Häkkinen, and H. Grönbeck, Phys. Rev. B **78**, 085426 (2008).
- ¹²M. Sterrer, T. Risse, U. Martinez Pozzoni, L. Giordano, M. Heyde, H.-P. Rust, G. Pacchioni, and H.-J. Freund, Phys. Rev. Lett. **98**, 096107 (2007).
- ¹³M. Sterrer, T. Risse, M. Heyde, H.-P. Rust, and H.-J. Freund, Phys. Rev. Lett. **98**, 206103 (2007).
- ¹⁴M. Kulawik, N. Nilius, and H.-J. Freund, Phys. Rev. Lett. **96**, 036103 (2006).
- ¹⁵N. Nilius, M. V. Ganduglia-Pirovano, V. Brázdová, M. Kulawik, J. Sauer, and H.-J. Freund, Phys. Rev. Lett. **100**, 096802 (2008).
- ¹⁶G. H. Vurens, M. Salmeron, and G. A. Somorjai, Surf. Sci. **201**, 129 (1988).
- ¹⁷Y. J. Kim, C. Westphal, R. X. Ynzunza, H. C. Galloway, M. Salmeron, M. A. Van Hove, and C. S. Fadley, Phys. Rev. B **55**, R13448 (1997).
- ¹⁸M. Ritter, W. Ranke, and W. Weiss, Phys. Rev. B **57**, 7240 (1998).
- ¹⁹E. D. L. Rienks, N. Nilius, H.-P. Rust, and H.-J. Freund, Phys. Rev. B **71**, 241404 (2005).
- ²⁰L. Giordano, G. Pacchioni, J. Goniakowski, N. Nilius, E. D. L. Rienks, and H.-J. Freund, Phys. Rev. B **76**, 075416 (2007).
- ²¹W. Zhang, Z. Li, Y. Luo, and J. Yang, J. Phys. Chem. C **113**, 8302 (2009).
- ²²N. Nilius, E. D. L. Rienks, H.-P. Rust, and H.-J. Freund, Phys. Rev. Lett. **95**, 066101 (2005).
- ²³L. Giordano, G. Pacchioni, J. Goniakowski, N. Nilius, E. D. L. Rienks, and H.-J. Freund, Phys. Rev. Lett. **101**, 026102 (2008).
- ²⁴U. Martinez, L. Giordano, and G. Pacchioni, J. Chem. Phys. **128**, 164707 (2008).
- ²⁵W. Zhao, G. Kerner, M. Asscher, X. M. Wilde, K. Al-Shamery, H.-J. Freund, V. Staemmler, and M. Wieszowska, Phys. Rev. B **62**, 7527 (2000).
- ²⁶J. Repp, G. Meyer, F. E. Olsson, and M. Persson, Science **305**, 493 (2004).
- ²⁷H. Grönbeck, J. Phys. Chem. B **110**, 11977 (2006).
- ²⁸A. Hellman and H. Grönbeck, Phys. Rev. Lett. **100**, 116801 (2008).
- ²⁹G. Barcaro, A. Fortunelli, and G. Granozzi, Phys. Chem. Chem. Phys. **10**, 1876 (2008).
- ³⁰J. Goniakowski and C. Noguera, Phys. Rev. B **79**, 155433 (2009).
- ³¹J. Goniakowski, C. Noguera, and L. Giordano, Phys. Rev. Lett. **93**, 215702 (2004).
- ³²S. L. Dudarev, G. A. Botton, S. Y. Savrasov, C. J. Humphreys, and A. P. Sutton, Phys. Rev. B **57**, 1505 (1998).
- ³³G. Kresse and J. Hafner, Phys. Rev. B **47**, 558 (1993).
- ³⁴G. Kresse and J. Furthmüller, Phys. Rev. B **54**, 11169 (1996).
- ³⁵J. P. Perdew, J. A. Chevary, S. H. Vosko, K. A. Jackson, M. R. Pederson, D. J. Singh, and C. Fiolhais, Phys. Rev. B **46**, 6671 (1992).
- ³⁶P. E. Blöchl, Phys. Rev. B **50**, 17953 (1994).
- ³⁷O. Bengone, M. Alouani, P. E. Blöchl, and J. Hugel, Phys. Rev. B **62**, 16392 (2000).
- ³⁸R. F. W. Bader, Chem. Rev. **91**, 893 (1991).
- ³⁹As implemented in the ABINIT code by K. Casek, F. Finocchi, and X. Gonze.
- ⁴⁰S. Prada, U. Martinez, and G. Pacchioni, Phys. Rev. B **78**, 235423 (2008).
- ⁴¹The computed value of the work function also depends on the lateral lattice constant: $\Phi(\text{MgO}/\text{Pt})=4.7$ eV and $\Phi(\text{Pt})=5.6$ eV at $a_{\text{latt}}=3.3$ Å; $\Phi(\text{FeO}/\text{Pt})=5.5$ eV and $\Phi(\text{Pt})=6.1$ eV at $a_{\text{latt}}=3.1$ Å, but $\Phi(\text{Pt})=5.8$ eV at Pt equilibrium lattice parameter $a_0=3.2$ Å. Thus, the strain in the Pt substrate, necessary to match the two lattices in the calculations, affects also Φ (oxide/metal). The result is an enhancement of the effect induced by the oxide film $\Phi(\text{MgO}/\text{Pt}) < \Phi(\text{FeO}/\text{Pt})$.
- ⁴²J. Goniakowski and C. Noguera, Interface Sci. **12**, 93 (2004).